



## DEVELOPMENT AND OPTIMIZATION OF SELF-COMPACTING CONCRETE MIXES: INSIGHTS FROM ARTIFICIAL NEURAL NETWORKS AND COMPUTATIONAL APPROACHES

P. Hosseini<sup>1,\*</sup>, A.Kaveh<sup>2</sup> and A.Naghian<sup>1</sup>

<sup>1</sup>*Faculty of Engineering, Mahallat Institute of Higher Education, Mahallat, Iran*

<sup>2</sup>*School of Civil Engineering, Iran University of Science and Technology, Tehran, Iran*

### ABSTRACT

In this study, experimental and computational approaches are used in order to develop and optimize self-compacting concrete mixes (Artificial neural network, EVPS metaheuristic algorithm, Taguchi method). Initially, ten basic mix designs were tested, and an artificial neural network was trained to predict the properties of these mixes. The network was then used to generate ten optimized mixes using the EVPS algorithm. Three mixes with the highest compressive strength were selected, and additional tests were conducted using the Taguchi approach. Inputting these results, along with the initial mix designs, into a second trained neural network, 10 new mix designs were tested using the network. Two of these mixes did not meet the requirements for self-compacting concrete, specifically in the U-box test. However, the predicted compressive strength results showed excellent agreement with low error percentages compared to the laboratory results, which indicates the effectiveness of the artificial neural network in predicting concrete properties, thus indicating that self-compacting concrete properties can be predicted with reasonable accuracy. The paper emphasizes the reliability and cost-effectiveness of artificial neural networks in predicting concrete properties. The study highlights the importance of providing diverse and abundant training data to improve the accuracy of predictions. The results demonstrate that neural networks can serve as valuable tools for predicting concrete characteristics, saving time and resources in the process. Overall, the research provides insights into the development of self-compacting concrete mixes and highlights the effectiveness of computational approaches in optimizing concrete performance.

**Keywords:** self-compacting concrete; Artificial Neural Networks; Optimization; Taguchi's Method; compressive strength; EVPS algorithm.

Received: 12 January 2023 Accepted: 23 May 2023

\*Corresponding author: Faculty of Engineering, Mahallat Institute of Higher Education, Mahallat, Iran

†E-mail address: p.hosseini@mahallat.ac.ir (P. Hosseini)

## 1. INTRODUCTION

A major goal of concrete specialists is to create concrete without the need for vibration by using additives and altering the ratios of components in the mix as well as eliminating the weaknesses of concrete caused by shaking and compaction. The result of these efforts was the invention of self-compacting concrete. Over the past few decades, researchers have focused on the advantages of self-compacting concrete, and they have sought to make concrete that fills molds without vibration. The definition of self-compacting concrete given by Bartos is concrete that flows under its own weight without any vibration and even with dense rebars, it is able to fully fill the molds and maintain its homogeneity [1]. In Japan, this concrete was initially developed in order to achieve durable structural concrete without requiring vibration to perform its function [2]. The following are some of the important advantages of this concrete:

Elimination of shaking operations, ease of pouring concrete, increased execution speed, ensuring proper compaction, especially in sections with high rebar density, optimal resistance against aggregate separation, smooth and beautiful final surfaces, reduced noise pollution in urban environments, and the ability to create smooth and beautiful final surfaces [3]. Since self-compacting concrete is widely used, optimizing its resistance using artificial neural networks is an interesting research topic. Unlike the classical methods available in statistical theories, the artificial neural network model does not require a specific model or function, as well as limiting assumptions to linearize the problem [4]. To date, many researchers have developed different models of artificial neural networks to predict the properties of different concretes, which is described below in the field of concrete technology. Oztas et al. [5] used artificial neural networks in 2006 to predict the compressive strength and slump of high strength concrete. The modulus of elasticity of normal and high strength concrete was predicted by Demir using an artificial neural network [6]. Using artificial neural networks, Rofooei et al. [7] presented a novel method for investigating seismic vulnerability of concrete structures with moment resisting frames (MRFs). The previous Iranian seismic design code, Standard 2800 (First Edition), was used to design a number of two-dimensional structural models with varying number of bays and stories. These structural models were subjected to extensive nonlinear dynamic analyses under a number of earthquake records in order to determine the seismically-induced damage they have sustained.

The artificial neural networks was utilized by Barbuta et al. [8] to predict the compressive strength and flexural strength of polymer concrete containing fly ash. According to Sonebi et al. [9], artificial neural networks were used to model self-compacting concrete's fresh properties. According to Kaveh et al. [10], various machine learning techniques were employed to establish a correlation between the fiber angle and the buckling capacity of cylinders when subjected to bending-induced loads. There are approximately 11,000 cases in the data set, containing seven attributes for 11 aspect ratios. Based on the numerical results, it can be concluded that the Deep Learning model achieves stable results with smaller errors and higher generalization compared to Random Forest Regression, Decision Tree algorithm, and Multiple Linear Regression [10]. A combination of meta-heuristic algorithms and two different types of artificial neural network structures was used by Kaveh and Khavanizadeh [11] to optimize the parameters of feed forward backpropagation and radial basis function

networks by using several metaheuristic algorithms. Training and test data sets were generated using 223 test data on Carbon FRP (CFRP) collected from the available literature, and various validation criteria were used to verify the models, including mean square errors, root mean square errors, and correlation coefficients (R). Hosseini et al. [12] used artificial neural networks to predict concrete's compressive strength, which can be increased simply by altering aggregate properties without affecting water or cement content; they used metaheuristic algorithms which can be applied to artificial neural networks efficiently and effectively. Beskopylny et al. [13] used a planetary ball mill to grind the components into a finely dispersed state and a particle analyzer to measure the particle size distribution. Microsilica increased concrete strength by 30% on the outside. It is defined by the American Concrete Institute (ACI 116R) as amorphous silica produced in electric arc furnaces as a byproduct of the production of silicon alloys or silicon metal. Gray powdered microsilica is somewhat similar to Portland cement or fly ash, which is an excellent application of microsilica as a microscopic distance reducer between aggregate and cement paste in concrete. It is important to note that by using them, the transition zone gap is minimized, and concrete is strengthened and has better physical properties. Taguchi's method can be used in conjunction with artificial neural networks due to the large number of design variables and simultaneous use of these parameters. As a method, the Taguchi method optimizes the level of parameters affecting all types of experiments. In fact, this method is presented as a tool for improving the quality of products by applying statistical and engineering concepts. In order to achieve the design goals with the smallest number of tests, the trial and error method is generally time-consuming and costly. Taguchi's approach involves consciously changing the input variables in order to identify the amount of change in the process response. Therefore, by systematically changing the input factors, the effects of these changes can be evaluated on the output parameters. Using the Taguchi method, Teimortashlu et al. were able to optimize the compressive strength of self-consolidating tertiary blend mortars. Three factors were identified at four levels and experiments were conducted on samples using a L16 design to determine the optimal factor levels [14]. Using the Taguchi method, Mohini et al. [15] investigated the design of self-compacting concrete mixtures with high strength. As factors or influencing factors in the design of self-compacting concrete mix with high strength and the best mix design obtained for high strength and less presence of absorbed air, they considered the ratio of water to cement, the amount of water, the percentage of fine aggregate to total aggregate, the amount of fly ash, the air absorption factor, and the amount of superplasticizers. Side et al. [16] optimized the mortar mix design by using the Taguchi method to determine the amount of cement to be replaced with silica fume and obtained the compressive strength of cubic samples measuring 5 x 5 x 5 cm. Based on the results of the study, the optimal ratio for the mixture design was 150 grams of silica fume, 660 grams of cement, and 1400 grams of sand. Thus, 18.52 percent of cement was replaced by silica fume, and its compressive strength measured 54 MPa, pH was 9.75, and water absorption measured 5.369%. According to this study, the authors have considered the basic designs for self-compacting concrete, and these designs have passed all tests related to self-compacting concrete, as well as their compressive strength. In the following, an artificial neural network was trained with the results of the basic designs, and optimization operations were conducted using EVPS meta-heuristic algorithm. Several limited designs were selected as favored designs from the artificial neural

network, and a similar approach was used to select some designs using the Taguchi method. Then, optimized designs of artificial neural networks and suggested Taguchi method were subjected to self-compacting concrete tests, and designs which failed to obtain good results were discarded, and the 28-day compressive strength of other designs was determined. Design variables included the aggregate size, the amount of cement, and the amount of water and additives. Using the results of the basic designs and the new results, an artificial neural network was trained again in accordance with the procedure of the previous step. Based on the experimental results, the artificial neural network trained at this stage has an acceptable level of accuracy.

This study is introduced in the first section, followed by a brief discussion of the EVPS meta-heuristic algorithm, artificial neural network, and Taguchi method. In the third section, the laboratory program, materials, and consumables are discussed, concrete mix design specifications are provided, tests are conducted on fresh and hardened concrete, and the laboratory results are analyzed, and at the end of the paper, the discussion and conclusion are presented.

## **2. A BRIEF DISCUSSION OF THE EVPS META-HEURISTIC ALGORITHM, ARTIFICIAL NEURAL NETWORK, AND TAGUCHI METHOD**

### *2.1 The EVPS meta-heuristic algorithm*

Metaheuristic algorithms have gained considerable attention in engineering sciences due to their broad applicability. They offer versatile problem-solving approaches that can be applied to a wide range of engineering disciplines. The widespread use of metaheuristic algorithms in engineering is evident from numerous studies that have investigated their effectiveness and explored their applications in different engineering domains. These algorithms provide valuable tools for tackling complex engineering problems and finding optimal solutions [17-21].

In the field of structural engineering and design, the EVPS algorithm is widely used as an enhanced version of the VPS algorithm for optimizing problems related to structural engineering and design. A number of studies have been conducted on the EVPS algorithm as well as the procedures of it [22-26].

### *2.2 Artificial Neural Network (ANN)*

Artificial Neural Networks (ANNs) are computational models inspired by biological neural networks. They serve as intelligence tools, learning patterns and predicting outcomes in high-dimensional spaces. The performance of neural networks relies on the training process, which involves adjusting the network's weights and biases. This enables the network to accurately estimate the desired output for a given problem. Within each neuron, as depicted in Fig. 1, a weighted sum of inputs is computed, and an activation function is applied to this value along with a bias. Throughout the training phase, the network's weights and biases are iteratively modified to minimize the error between the target values (actual values) and the output values (network predictions) .

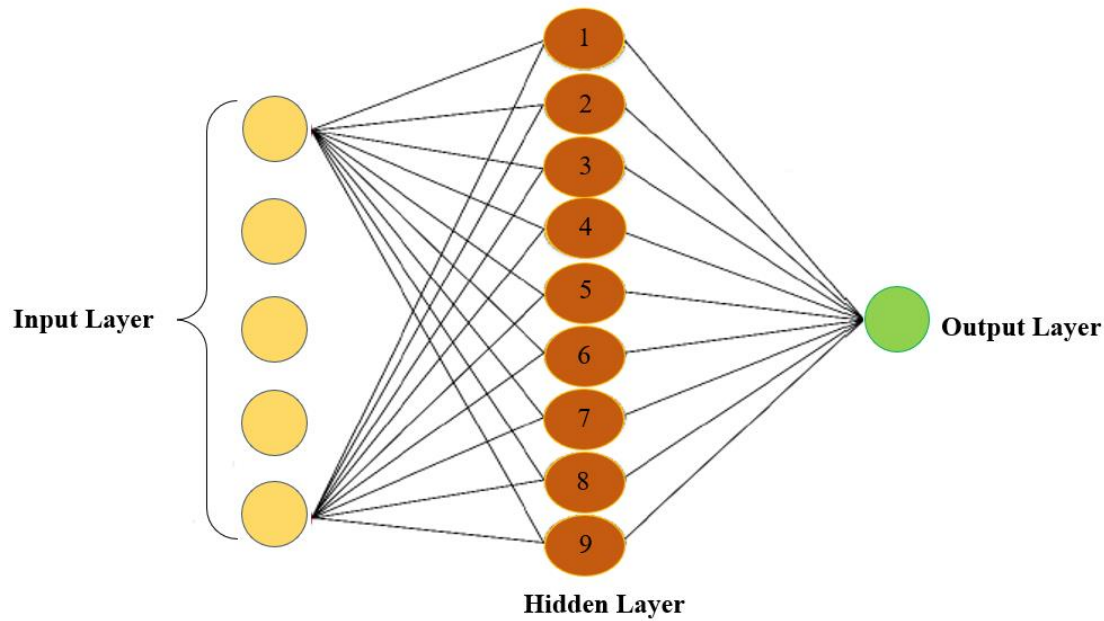


Figure 1. An ANN structure schematic showing an input layer, an output layer, and a hidden layer [12]

### 2.3 Taguchi method

Professor Genichi Taguchi introduced the Taguchi method in 1988 with the aim of achieving optimal combinations while minimizing the number of tests, reducing costs, and saving time. This approach considers the number of factors and test levels when analyzing various arrays. In Taguchi's method, signal-to-noise ratios are employed to analyze the results. The S/N value indicates how the results change over a specific number of tests, and based on the obtained results, the S/N ratio can be calculated using the following equations:

$$\begin{aligned} \frac{S}{N} &= -10 \log_{10} \left[ \frac{1}{n} \sum_{i=1}^n y_i^2 \right] && \text{Smaller the better} \\ \frac{S}{N} &= -10 \log_{10} \left[ \frac{1}{n} \sum_{i=1}^n \frac{1}{y_i^2} \right] && \text{Larger the better} \\ \frac{S}{N} &= -10 \log_{10} [\sigma^2] && \text{Nominal the better} \end{aligned} \quad (1)$$

where,  $y_i$  represents the value obtained for the  $i$ th response, and  $n$  denotes the number of trial repetitions. The signal-to-noise ratio reflects the impact of control factors on the response,

where a higher S/N value indicates a better response. Consequently, the optimal control levels are determined based on the setting of control factor levels that yield the highest S/N ratio.

Taguchi's philosophy is built on three fundamental concepts: quality should be designed rather than checked, minimizing deviations from specified values is the best way to achieve quality, and products must be designed to be resilient against uncontrollable environmental conditions.

The third part of the study mentions that the number of influential factors in this study is ten, and that each of them is examined at three levels. According to Table 1, an orthogonal array of L27 is used. In L27, 27 trials are required in order to analyze the data. It is recommended that 310 tests be performed if the Taguchi method is not used in order to perform a sensitivity analysis on the parameters.

Table 1. The selection of orthogonal arrays

|                      | The number of parameters |     |     |     |     |
|----------------------|--------------------------|-----|-----|-----|-----|
|                      | 6                        | 7   | 8   | 9   | 10  |
| The number of levels | L8                       | L12 | L16 | L32 | L16 |
|                      | L27                      | L27 | L27 | L27 | L27 |

### 3. THE LABORATORY PROGRAM

This section discusses the used materials, mixing plans, and tests of fresh and hardened SCC concrete, as well as their results.

#### 3.1 The utilized materials

For the purpose of this study, aggregate, cement, microsilica powder, and superplasticizer (the term additive will be used for simplicity) were used to construct concrete samples. The aggregates are passed through a sieve of 3/8 inch and the remaining aggregates are passed through a sieve of No. 4. The samples were made using Portland cement type 2 produced at Delijan City Cement Factory. For self-compacting concrete to achieve the desired efficiency, additives are required. Among the additive properties used, it is possible to mention such properties as increased concrete consistency, prevention of aggregate separation, better compaction, reduction of permeability, and reduced water to cement ratio.

#### 3.2 Specifications for concrete mix design

As a first step, some basic mixing designs containing microsilica for self-compacting concrete were proposed and tested in the laboratory. At the end, ten Basic Mixing Designs (BMD) were selected, whose specifications are given in Table 2. It is noteworthy that the ten selected designs had self-compacting conditions in the fresh concrete phase without bleeding and passed the self-compacting concrete experimental tests and achieved a satisfactory compressive strength in the hardened concrete phase. Different mix designs are used with the available materials in order to provide an economical mixing design for the construction of self-compacting concrete containing microsilica.

Table 2. Specifications for ten basic mix designs

| Mix design | Quantity of material (kg/m <sup>3</sup> ) |       |             |          |        |      |
|------------|---|-------|-------------|----------|--------|------|
|            | Cement                                    | Water | Microsilica | additive | Gravel | Sand |
| SCC/BMD1   | 619                                       | 224   | 62          | 4        | 619    | 934  |
| SCC/BMD2   | 580                                       | 210   | 87          | 7        | 641    | 961  |
| SCC/BMD3   | 578                                       | 202   | 58          | 6        | 548    | 1066 |
| SCC/BMD4   | 607                                       | 220   | 61          | 7        | 607    | 960  |
| SCC/BMD5   | 600                                       | 217   | 60          | 7        | 626    | 950  |
| SCC/BMD6   | 571                                       | 235   | 57          | 4        | 631    | 960  |
| SCC/BMD7   | 590                                       | 206   | 59          | 6        | 501    | 1097 |
| SCC/BMD8   | 534                                       | 193   | 53          | 6        | 589    | 1077 |
| SCC/BMD9   | 519                                       | 213   | 52          | 3        | 605    | 1060 |
| SCC/BMD10  | 515                                       | 212   | 51          | 6        | 575    | 1093 |

### 3.3 A selection of three Taguchi method designs

Table 3 presents three selected proposed mixing designs for the Taguchi method. Taguchi's numerical and graphical analysis indicates that fine aggregate, cement content, water, and admixture are the factors that influence workability and quality of self-compacting concrete. The quality and performance of self-compacting concrete can be improved by controlling and utilizing the properties of each variable intelligently. Experiments conducted in the laboratory support this observation.

Table 3. Three selected proposed mixing designs for the Taguchi method

| Mix design | Quantity of material (kg/m <sup>3</sup> ) |       |             |          |        |      |
|------------|---|-------|-------------|----------|--------|------|
|            | Cement                                    | Water | Microsilica | additive | Gravel | Sand |
| T1         | 619                                       | 224   | 62          | 4        | 619    | 934  |
| T2         | 580                                       | 210   | 87          | 7        | 641    | 961  |
| T3         | 578                                       | 202   | 57          | 6        | 548    | 1066 |

### 3.4 Construction and Preparation

In order to prepare the mixtures, the required materials must first be accurately weighed. Next, the measured sand and gravel are poured into an electric mixer, and the cement is added to the mixture and mixed for one minute. In the following stage, 10% of the cement's weight is added as microsilica and another minute of mixing is carried out. In the next stage, half of the mixing water is added to the mixer, and the mixture is blended for one minute. In the final stage, the remaining water and superplasticizer are thoroughly mixed and added to the mixer, and the mixing operation continues for three minutes. A self-compaction test is conducted immediately following the mixing of the mixture, followed by the casting of the samples and the removal of the samples after 24 hours. The samples are stored in a water basin at a temperature between 19 and 23 degrees Celsius. For sample preparation and sample processing, it is advisable to use the same water [27].

### 3.5 Self-compacting concrete experiments

Some experiments related to self-compacting concrete have been selected as the fundamental tests in order to evaluate the self-compacting properties of the samples produced. In addition to the J-ring test, the V-funnel test, the L-box test, and the U-box test, Slump flow test, compressive strength and flexural strength tests are required.

#### 3.5.1 L-box test

As described in EN 12350-10:20, the L-box test is used to assess the passability and flow characteristics of self-compacting concrete. This test measures the flowability of concrete mixtures as they pass through an L-shaped box apparatus. There are two perpendicular sections in the L-box, with one section being narrower than the other. In the narrower section, concrete is poured, and the time it takes for the concrete to flow through and fill the wider section is recorded. During this test, concrete is evaluated for its ability to flow and fill complex shapes and congested reinforcement areas [28]. Approximately 14 liters of concrete are poured into an L-shaped box, and after one minute, the gate is opened, and the timing begins. Concrete passes through the steel bars and enters the horizontal section of the box. The time taken for the concrete to reach 200 and 400 millimeters along the horizontal section of the box is recorded in order to determine the viscosity of the concrete. A blocking ratio can be calculated by measuring the height of the concrete in the vertical section (H1) and the height of the concrete at the end of the horizontal section (H2). The closer the concrete's flowability is to ideal, the closer the heights H1 and H2 will be to each other, resulting in a close blocking ratio. Conversely, as the flowability of the concrete decreases, the blocking ratio decreases.

##### 3.5.1.1 Results of L-Box Test

Table 4 presents the results of the L-Box test, and it should be noted that the acceptable range for the (H2/H1) ratio lies between 0.8 and 1 [29, 30]. When the ratio is closer to one, it indicates equal height of concrete in the two regions, indicating the concrete can pass through the reinforcement and exhibits satisfactory performance. Based on the results shown, all designs are within the acceptable range. Additionally, two cases that failed the test and were predicted by the artificial neural network based on the initial design are included. Fig. 2 illustrates the time comparison between L200 and L400 in the L-Box test

Table 4. Results of L-Box Test

| Mix design | H1   | H2   | H2/H1 | Acceptable range | Result |
|------------|------|------|-------|------------------|--------|
|            | (cm) | (cm) |       |                  |        |
| SCC/BMD1   | 8.62 | 8.62 | 1     | 0.8-1            | ok     |
| SCC/BMD2   | 9.02 | 9.02 | 1     | 0.8-1            | ok     |
| SCC/BMD3   | 9.02 | 9.02 | 1     | 0.8-1            | ok     |
| SCC/BMD4   | 8.74 | 8.74 | 1     | 0.8-1            | ok     |
| SCC/BMD5   | 8.27 | 8.27 | 1     | 0.8-1            | ok     |
| SCC/BMD6   | 9.17 | 9.17 | 1     | 0.8-1            | ok     |
| SCC/BMD7   | 8.65 | 8.65 | 1     | 0.8-1            | ok     |



|           |       |       |      |       |        |
|-----------|-------|-------|------|-------|--------|
| SCC/BMD8  | 8.11  | 8.11  | 1    | 0.8-1 | ok     |
| SCC/BMD9  | 9     | 8.74  | 0.97 | 1-0.8 | ok     |
| SCC/BMD10 | 10.23 | 8.35  | 0.82 | 1-0.8 | ok     |
| ANN1      | 7.16  | 10.84 | 1.51 | 0.8-1 | Not ok |
| ANN2      | 7.66  | 10.34 | 1.35 | 0.8-1 | Not ok |

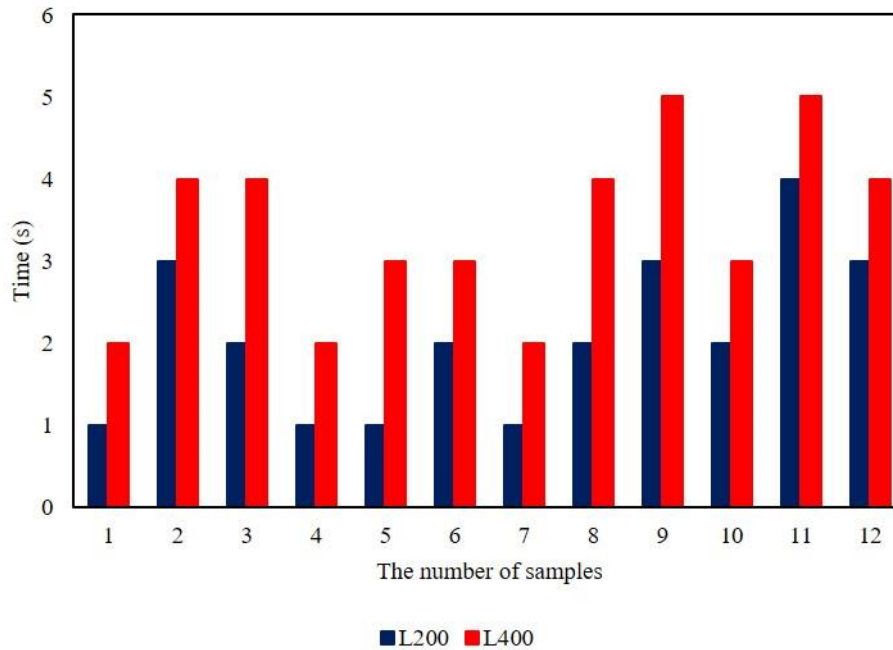


Figure 2. Comparison of Time for L200 and L400 in L-Box Test

### 3.5.2 U-box test

According to the UNI 11044 standard, the U-Box test evaluates the flowability and passing ability of self-compacting concrete [31]. A U-shaped box apparatus is used for this test, which consists of two vertical arms connected by a horizontal section. In order to conduct the U-Box test, a specified volume of self-compacting concrete is poured into a U-shaped box. In order to fill the horizontal section, concrete is allowed to flow through the arms. The concrete's ability to pass the arms is measured by the time it takes for it to reach specific marks along the arms. U-Box tests provide valuable information regarding the ability of self-compacting concrete to flow and pass through tight spaces, such as congested reinforcement or narrow gaps. Test results can be used to optimize mixture proportions and ensure the desired workability and performance of concrete. A U-Box test is an important tool for assessing the suitability of self-compacting concrete for various construction applications, particularly in those requiring high flowability and good passability. The interior surface of the U-shaped box has been moistened, and the lower gate of the box has been closed. The left side of the box is then filled with approximately 20 liters of concrete. Upon removing the middle movable plate, the concrete will flow from the left side of the box to the right side after one minute. After the concrete has ceased flowing, the height of the concrete is

measured on both sides of the box and labelled as parameters H1 and H2. Filling height difference is calculated as the difference in height between these two values. The closer the filling height difference to zero, the better the flowability of the concrete will be. [32]

### 3.5.2.1 Results of U-Box Test

Based on Table 5, the results can be interpreted by determining the height difference between the two compartments. The closer the height difference between the concrete in the two compartments is to zero, the more fluid and passable the concrete will be. Alternatively, as this value increases, the viscosity of the concrete also increases, increasing the likelihood of a blockage. In the case of self-compacting concrete, the maximum height difference between the two compartments should not exceed three centimeters. [32]

Table 5. Results of U-Box Test

| Mix design | H1<br>(cm) | H2<br>(cm) | H1-H2<br>(cm) | Acceptable range<br>(cm) | Result |
|------------|------------|------------|---------------|--------------------------|--------|
| SCC/BMD1   | 29.5       | 29.5       | 0             | 0-3                      | ok     |
| SCC/BMD2   | 29         | 29         | 0             | 0-3                      | ok     |
| SCC/BMD3   | 28.9       | 28.9       | 0             | 0-3                      | ok     |
| SCC/BMD4   | 28.4       | 28.4       | 0             | 0-3                      | ok     |
| SCC/BMD5   | 29.4       | 29.4       | 0             | 0-3                      | ok     |
| SCC/BMD6   | 28.6       | 28.6       | 0             | 0-3                      | ok     |
| SCC/BMD7   | 28.5       | 28.5       | 0             | 0-3                      | ok     |
| SCC/BMD8   | 31.4       | 29.5       | 1.9           | 0-3                      | ok     |
| SCC/BMD9   | 28.65      | 27.46      | 1.19          | 0-3                      | ok     |
| SCC/BMD10  | 29.32      | 27.34      | 1.98          | 0-3                      | ok     |
| ANN1       | 33.02      | 28.9       | 4.12          | 0-3                      | Not Ok |
| ANN2       | 31.1       | 27.9       | 3.2           | 0-3                      | Not Ok |

### 3.5.3 V-funnel test

In order to evaluate the flowability and workability of self-compacting concrete, the V-funnel test is conducted. A V-shaped funnel is filled with the concrete mixture, and the time it takes for the concrete to flow through the funnel is measured. It is necessary to place the V-funnel on a flat surface and close the bottom outlet of the funnel. The concrete mixture is then poured into the funnel without being compacted. Upon removing the stopper from the bottom outlet, the concrete is allowed to flow out of the funnel for a specified period of time. The flow time obtained from the V-funnel test provides an indication of the self-compacting concrete's viscosity and flowability. Flow times that are shorter indicate better flowability, indicating that the concrete is able to flow easily and fill intricate spaces without requiring external compaction. Conversely, longer flow times may indicate a higher viscosity and reduced flowability, which may require additional compaction efforts. In order to ensure that self-compacting concrete is suitable for construction applications, the V-funnel test is widely used to assess its flow properties. As a measure of concrete segregation, this test can be used. As well as the time taken for concrete to flow out, which is measured in this test, the manner in which concrete flows through the funnel and the uniformity of the discharged

concrete are also important factors to consider. This device can also provide a visual indication of the homogeneity of the concrete. The inner surfaces of the V-shaped funnel are moistened after it has been placed on its stand. It is then filled with 12 liters of concrete, and after 10 seconds, the bottom outlet of the funnel is opened, allowing the concrete to flow out by its own weight. It is recorded how long it takes for the concrete to flow out of the funnel. Self-compacting concrete should be discharged through the V-funnel device within six to twelve seconds. It should be noted, however, that this parameter alone is not conclusive. A number of self-compacting concretes with discharge times less than 6 seconds or greater than 12 seconds have also been successfully applied. Generally, if the discharge time exceeds 12 seconds, it indicates high plastic viscosity, while if the discharge time is less than 6 seconds, it indicates low viscosity and a likelihood of segregation. [33]

#### 3.5.4 J-ring test

According to ASTM C1621, the J-ring test is conducted to determine the passing ability and segregation resistance of self-compacting concrete [34]. In this test, a specially designed J-ring is placed on a flat surface and filled with self-compacting concrete. J-rings are composed of a cylindrical section and an outward-extending J-shaped section. The J-ring is filled with concrete and then vibrated to ensure proper compaction. The excess concrete is then removed from the top of the J-ring, and the height of the concrete inside the J-ring is determined. Following the initial height, the J-ring is lifted vertically by applying a gentle upward force, while ensuring the base remains in contact with the concrete. When the J-ring is gradually lifted, the concrete flows out from underneath the J-shaped section, which is known as the "slump flow height.". This height of concrete passing through the J-ring is known as the "J-ring flow height". Slump flow height and J-ring flow height provide an indication of the self-compacting concrete's ability to pass. Generally, a smaller difference indicates a better ability to pass and less susceptibility to segregation. Alternatively, a greater difference indicates a reduced ability to pass and an increased risk of segregation. In accordance with ASTM C1621, the J-ring test provides a standardized method for evaluating the ability of self-compacting concrete to flow through restricted sections. As a result, concrete is better able to fill formwork, penetrate dense reinforcement, and maintain homogeneity during placement. It is possible for engineers and contractors to assess whether self-compacting concrete is suitable for specific construction applications and make necessary adjustments in order to optimize its performance by conducting the J-ring test. Table 5 presents the results of the J-ring experiment

#### 3.5.5 Slump Flow test

The slump flow test is conducted to evaluate the flowability and consistency of self-compacting concrete, following the guidelines of ASTM C1611/C1611M [35]. It measures the ability of the concrete mixture to flow and spread freely without segregation or excessive resistance. In this test, a slump cone is filled with self-compacting concrete in a single lift, without any compaction or vibration. The cone is then slowly lifted vertically, allowing the concrete to flow out and spread on the base plate. The diameter of the concrete spread is measured in two perpendicular directions, and the average value is calculated. The measured diameter of the concrete spread provides an indication of the slump flow of the self-

compacting concrete. A larger diameter indicates better flowability, as the concrete is able to spread over a wider area. On the other hand, a smaller diameter suggests reduced flowability and potential issues with filling formwork or penetrating congested reinforcement. The slump flow test, according to ASTM C1611/C1611M, is an important tool for assessing the workability and flow properties of self-compacting concrete. It helps ensure that the concrete can easily flow and fill complex shapes and structures, while maintaining its homogeneity and avoiding segregation. By conducting the slump flow test, engineers and contractors can make informed decisions regarding the selection and adjustment of materials to achieve the desired flow characteristics of self-compacting concrete. Table 6 presents the results of the test.

Table 6. The results of the J-ring and slump flow tests

| Mix design | Slu        | J-ring | Acceptable range | Result |
|------------|------------|--------|------------------|--------|
|            | mp<br>(cm) |        |                  |        |
| SCC/BMD1   | 62         | 1.1    | >60              | ok     |
| SCC/BMD2   | 66         | 1.2    | >60              | ok     |
| SCC/BMD3   | 70         | 0.83   | >60              | ok     |
| SCC/BMD4   | 68         | 0.74   | >60              | ok     |
| SCC/BMD5   | 77         | 0.7    | >60              | ok     |
| SCC/BMD6   | 65         | 1.2    | >60              | ok     |
| SCC/BMD7   | 79         | 0.65   | >60              | ok     |
| SCC/BMD8   | 67         | 0.9    | >60              | ok     |
| SCC/BMD9   | 63         | 1      | >60              | ok     |
| SCC/BMD10  | 60         | 1.4    | >60              | ok     |

### 3.5.6 The compressive strength test

A compressive strength test, conducted in accordance with BS 1881, is a commonly conducted test to determine the strength of concrete [36]. A cylindrical or cubical specimen of concrete is prepared and subjected to a compressive load until failure occurs. The compressive strength of concrete is calculated by dividing the maximum load applied to the specimen by its cross-sectional area. The purpose of this test is to assess the structural integrity and load-bearing capacity of concrete in various construction applications. In order to ensure the quality and durability of concrete structures, the results of the compressive strength test are crucial. The compressive strength of cubic specimens with dimensions of 10x10x10 centimeters was tested at the age of 28 days in this study. In a water tank, specimens were prepared. Failure of a concrete specimen is illustrated in Fig. 3, a stress-strain curve is illustrated in Fig. 4 for one of the basic mix designs, and a compression strength chart is illustrated in Fig. 5 for each of the 10 basic mix designs.



Figure 3. Failure of a concrete specimen

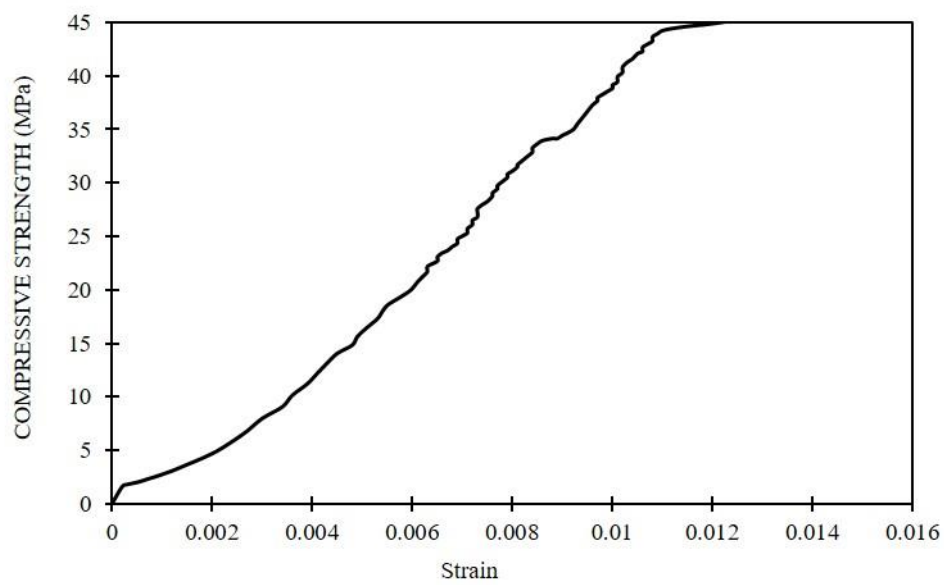


Figure 4. One of the basic design's stress-strain curve

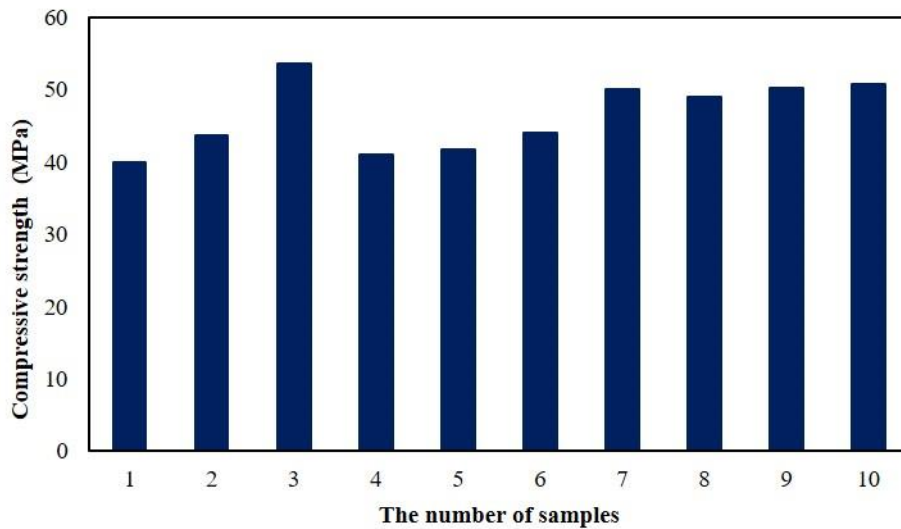


Figure 5. Compressive strength for the 10 basic mix designs

### 3.5.7 Flexural strength test

In the flexural strength test of concrete, the tensile strength of the concrete is indirectly measured. The purpose of this test is to measure the strength of concrete against bending. Concrete is typically tested for flexural strength using either the three-point loading method (ASTM C78) or the center-point loading method (ASTM C293). The three-point loading method was used in this study. [37, 38]

#### 3.5.7.1 Results of Flexural Strength Test

As a result of conducting the three-point flexural test on concrete beam specimens based on 10 basic mix designs, Fig. 6 illustrates the results of the three-point flexural test when applied at the center of the span. Furthermore, Fig. 7 illustrates a broken concrete beam during a flexural strength test.

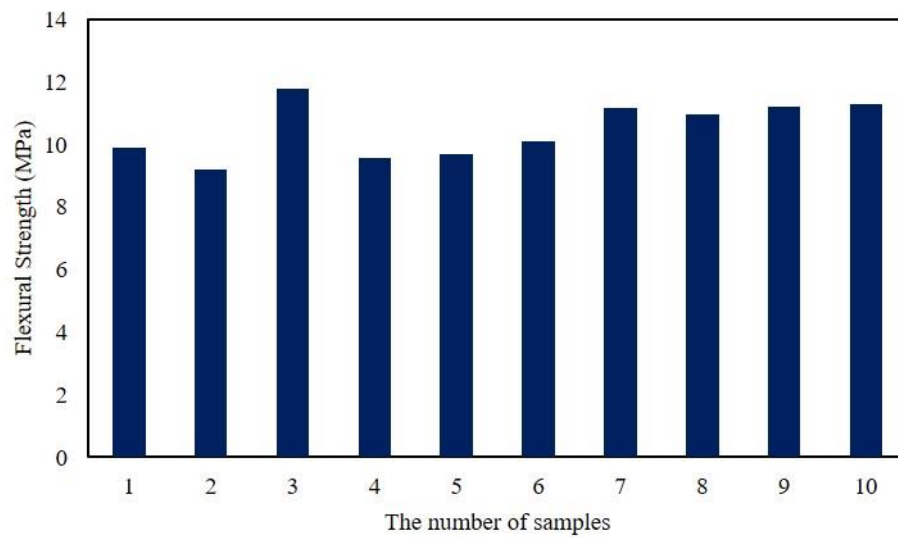


Figure 6. Three-point flexural test on concrete beam specimens using 10 basic mix designs



Figure 7 Broken concrete beam during a flexural strength test

### 3.5.8 Test Results of 10 Basic Mix Designs, Taguchi-Based Selections, and Optimal Artificial Neural Network Outcomes

The results of the tests conducted on the ten basic mix designs, as well as three selected designs based on the Taguchi method and the best results from the artificial neural networks that yielded the best results, are presented in Table 7. In this table, the results of the J-ring and V-funnel tests are provided as a range for the 10 basic mix designs and three selected designs based on the Taguchi method. Additionally, two of the best results from the initial artificial neural network (in the first training) and three of the best results from the second

artificial neural network (in the second training) were considered.

Table 7. Test results on the 10 basic mix designs, as well as three selected designs based on the Taguchi method as well as the best results from the artificial neural networks (ANNs).

| Mix design | Fresh Concrete |          |                         |       | Hardened Concrete                                 |                    |
|------------|----------------|----------|-------------------------|-------|---|--------------------|
|            | J-ring         | V-funnel | U-box Test (Difference) | L-box | 28-day Compressive Strength (kg/cm <sup>2</sup> ) |                    |
|            | (mm)           | (sec)    | (mm)                    | (mm)  | Experimental Results                              | The ANN Prediction |
| SCC/BMD1   | 60-120         | 5-9      | 0                       | 1     | 407   | 447                |
| SCC/BMD2   |                |          | 0                       | 1     | 446   | 454                |
| SCC/BMD3   |                |          | 0                       | 1     | 524   | 498                |
| SCC/BMD4   |                |          | 0                       | 1     | 418   | 448                |
| SCC/BMD5   |                |          | 0                       | 1     | 424   | 400                |
| SCC/BMD6   |                |          | 0                       | 1     | 449   | 460                |
| SCC/BMD7   |                |          | 0                       | 1     | 509   | 550                |
| SCC/BMD8   |                |          | 0                       | 1     | 500   | 472                |
| SCC/BMD9   |                |          | 0                       | 1     | 512   | 563                |
| SCC/BMD10  |                |          | 0                       | 1     | 516   | 527                |
| TAGUCHI1   | 80-100         | 6-8      | 0                       | 1     | 475   | 451                |
| TAGUCHI2   |                |          | 0                       | 1     | 411   | 439                |
| TAGUCHI3   |                |          | 0                       | 1     | 457   | 521                |
| ANN1-1     | 70-90          | 9-11     | 0                       | 1     | 481   | 500                |
| ANN1-2     |                |          | 0                       | 1     | 445   | 454                |
| ANN2-1     | 70-90          | 9-11     | 0                       | 1     | 475   | 470                |
| ANN2-2     |                |          | 0                       | 1     | 437   | 446                |
| ANN2-3     |                |          | 0                       | 1     | 397   | 391                |

#### 4. DISCUSSION

Ten basic mix designs were initially tested for self-compacting concrete, compressive strength, and flexural strength. Based on the gradation of aggregates, the amount of cement, water, and additives, ten factors were taken into account as effective design variables on the test results. Based on the ten basic mix designs, an artificial neural network was trained and ten optimized mixes were extracted using the EVPS algorithm based on the initial trained neural network. The mixes were then tested according to the tests listed above and three mixes were selected with the highest compressive strength while the results of the other tests were acceptable. In addition, 27 additional tests were conducted using the Taguchi approach with ten design variables. Without the Taguchi method, it would require a large number of samples with combinations of ten base mixes, which is practically impossible.

As a result of failing certain tests, some of the Taguchi results were discarded, and the remaining results from the Taguchi method, the initial ten basic mix designs, and the three



top mixes from the initial neural network were then input into the neural network. It was observed that the predicted results differ slightly from the laboratory results, indicating that the trained network has achieved a reasonable level of accuracy. During the training of the neural network, the more data with greater diversity that are provided, the better the network learns, and the closer the prediction results will be to the laboratory results. Consequently, artificial neural networks can be regarded as reliable and cost-effective tools that provide significant predictive power for the intended issues, as well as saving time and resources. Fig. 8 illustrates the comparison between the laboratory results and the predictions made by the second trained artificial neural network.

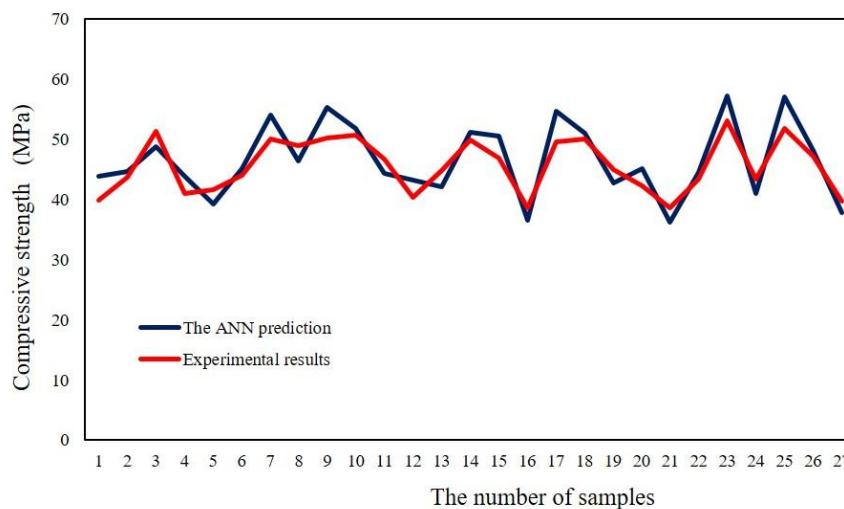


Figure 8. The comparison between the laboratory results and the predictions made by the second trained artificial neural network

## 5. CONCLUDING REMARKS

This research highlights the reliability and cost-effectiveness of using artificial neural networks (ANNs), the EVPS metaheuristic algorithm, and the Taguchi method in predicting concrete properties. By leveraging diverse training data, the ANNs demonstrate their ability to accurately predict concrete properties, saving valuable time and resources in the process. The EVPS metaheuristic algorithm further contributes to the optimization of concrete performance, enabling the generation of superior mix designs with improved properties.

Additionally, the application of the Taguchi method complements the computational approaches by providing a systematic and efficient experimental approach for selecting and evaluating mix designs. By considering factors such as the J-ring test, V-funnel test, L-box test, U-box test, slump flow test, compressive strength, and flexural strength tests, the study ensures a comprehensive evaluation of the self-compacting properties of the concrete samples. Together, these computational and experimental approaches offer valuable insights into the development and optimization of self-compacting concrete mixes. The findings emphasize the effectiveness of using ANNs, the EVPS metaheuristic algorithm, and the

Taguchi method in achieving accurate predictions and improving concrete performance. The research serves as a foundation for future advancements in the field, paving the way for more efficient and reliable construction practices.

### ACKNOWLEDGMENT

We would like to express our sincere gratitude to Mahallat Institute of Higher Education for the generous support and provision of laboratory equipment. Their contribution has greatly enhanced our research capabilities and has been instrumental in the successful completion of our experiments. We are deeply grateful for their commitment to promoting academic excellence and their dedication to fostering a conducive learning environment. The valuable resources provided by Mahallat Institute of Higher Education have played a crucial role in advancing our scientific endeavors, and we extend our heartfelt appreciation for the unwavering support.

### REFERENCES

1. Bartos PJM, Gibbs JC, Zhu W. Uniformity of in Situ Properties of Self- Compacting Concrete in Full Scale Structural Elements. *Cement Concrete Compos* 2001; **23**(1): 57-64
2. Okamura H, Ouchi M. Self-compacting concrete. *J Adv Concrete Technol* 2003; 1(1), 5-15
3. Dehwah HAF. Mechanical properties of self-compacting concrete incorporating quarry dust powder, silica fume or fly ash. *Construct Build Mater* 2012; **26**: 547-51
4. Kaveh, A., & Khalegi, A. (1998), Prediction of strength for concrete specimens using artificial neural network, *Asian Journal of Civil Engineering*, 2(2), 1-13.
5. Oztas A, Pala M, Ozbay E, Kanca E, Caglar N, Bhatti M.A. Predicting the compressive strength and slump of high strength concrete using neural network. *Construct Buil Mater* 2006; **20**(9): 769–75
6. Demir F. Prediction of elastic modulus of normal and high strength concrete by artificial neural networks. *Construct Build Mater* 2008; **22**(7): 1428–35
7. Rofooei F, Kaveh A, Farahani F. Estimating the vulnerability of the concrete moment resisting frame structures using artificial neural networks. *Int J Optim Civil Eng* 2011; **1** (3): 433-48
8. Barbuta M, Diaconescu RM, Harja M. Using Neural Networks for Prediction of Properties of Polymer Concrete with Fly Ash. *J Mater Civil Eng* 2012; **24**(5): 523-8
9. Sonebi M, Grünwald S, Cevik A, Walraven J. Modelling fresh properties of self-compacting concrete using Neural network technique. *Comput Concrete* 2016; **18**(4), 903-20
10. Kaveh A, Dadras Eslamlou A, Javadi SM, Geran Malek N. Machine learning regression approaches for predicting the ultimate buckling load of variable-stiffness composite cylinders. *Acta Mech* 2021; **232**, 921–31.
11. Kaveh A, Khavaninzadeh N. Efficient training of two ANNs using four meta-heuristic algorithms for predicting the FRP strength. *Structures* 2023; **52**: 256-72.

12. Hosseini P, Kaveh A, Naghian A. The use of artificial neural networks and metaheuristic algorithms to optimize the compressive strength of concrete. *Int J Optim Civl Eng* 2023; **13**(3): 327-38
13. Beskopylny A, Stel'makh SA, Shcherban E.M, Mailyan L.R, Meskhi B. Nano modifying additive micro silica influence on integral and differential characteristics of vibrocentrifuged concrete. *Journal of Building Engineering* 2022; **51**: 104235
14. Teimortashlu E, Dehestani M, Jalal M. Application of Taguchi method for compressive strength optimization of tertiary blended self-compacting mortar. *Construct Build Mater* 2018; **190**: 1182-91
15. Mohini U, Modani P.O, Gadewar AS. Study of Self Compacting Concrete - A Review. *Int Res J Eng Technol (IRJET)* 2019; **6**(3)
16. Jagadesh P, Prado-Gil J, Silva-Monteiro N, Martínez-García R. Assessing the compressive strength of self-compacting concrete with recycled aggregates from mix ratio using machine learning approach. *J Mater Res Technol* 2023; **24**: 1483-98
17. Kaveh A, Zakian P. Enhanced bat algorithm for optimal design of skeletal structures *Asian J Civil Eng* 2014; **15** (2): 179-212
18. Kaveh A, Rahami H, Analysis, design and optimization using force method and genetic algorithm", *Int J Numer Methods Eng.* 2006; **65**: 1570-84,
19. Kaveh A, Talatahari S. A charged system search with a fly to boundary method for discrete optimum design of truss structures, *Asian J Civil Eng* 2010; **11** (3): 277-93.
20. Kaveh A. Improved cycle bases for the flexibility analysis of structures, *Comput Methods Appl Mech Eng* 1976; **9** (3): 267-72.
21. Kaveh A, Kalateh-Ahani M, Fahimi-Farzam M, Constructability optimal design of reinforced concrete retaining walls using a multi-objective genetic algorithm, *Struct Eng Mech* 2013; **47**(2): 227-45
22. Hosseini P, Hoseini Vaez SR, Fathali MA, Mehanpour H. Reliability assessment of transmission line towers using metaheuristic algorithms. *Int J Optim Civl Eng* 2020; **10**(3): 531-51
23. Kaveh A, Hoseini Vaez SR, Hosseini P, Abedini H. Weight minimization and energy dissipation maximization of braced frames using EVPS algorithm. *Int J Optim Civl Eng* 2020; **10**(3): 513-29
24. Paknahad M, Hosseini P, Kaveh A. A self-adaptive enhanced vibrating particle system algorithm for continuous optimization problems. *Int J Optim Civl Eng* 2023; **13**(1): 127-42
25. Paknahad M, Hosseini P, Hakim SJS. SA-EVPS algorithm for discrete size optimization of the 582-bar spatial truss structure. *Int J Optim Civl Eng* 2023; **13**(2): 207-17
26. Kaveh A, Hoseini Vaez SR, Hosseini P. Enhanced vibrating particles system algorithm for damage identification of truss structures. *Scient Iranica* 2019; **26**(1): 246-56
27. ASTM C192/C192M-19, Standard Practice for Making and Curing Concrete Test Specimens in the Laboratory. American Society of Testing Materials 2019
28. EN, B., Testing Fresh Self-compacting Concrete, L-box test 2010
29. Mastali M, Dalvand A, Sattarifard A. The impact resistance and mechanical properties of reinforced self-compacting concrete with recycled glass fiber reinforced polymers. *J Cleaner Product* 2016; **124**: 312-24
30. Hama S, Hilal N. Fresh properties of self-compacting concrete with plastic waste as

- partial replacement of sand. *Int J Sustainable Built Environm* 2017; **6**(2), 299-308
31. UNI (Ente Nazionale Italiano di Unificazione). Testing fresh self compacting concrete: Determination of confined flowability in U-shape box. UNI 11044. 2010.
  32. Yaseri S, Mahdikhani M, Jafarinoor A, Masoomi VV, Esfandyari M, Ghiasian SM. The development of new empirical apparatuses for evaluation fresh properties of self-consolidating mortar: Theoretical and experimental study. *Construct Build Mater* 2018; **167**, 631-48
  33. BS EN 12350-9. Testing fresh concrete. Self-compacting concrete. V-funnel test 2010.
  34. ASTM C1621 / C1621M – 17. Standard Test Method for Passing Ability of Self-Consolidating Concrete by J-Ring, 2017
  35. ASTM C1611/C1611M – 18. Standard Test Method for Slump Flow of Self-Consolidating Concrete, 2018
  36. BS 1881-116. Testing concrete. Method for determination of compressive strength of concrete cubes 1983.
  37. ASTM C78-09. Standard Test Method for Flexural Strength of Concrete (Using Simple Beam with Third-Point Loading)
  38. ASTM C293/C293M-16. Standard Test Method for Flexural Strength of Concrete (Using Simple Beam With Center-Point Loading)